CHARACTERIZATION OF GHOSTING DEFECTS IN ELECTROPHOTOGRAPHIC PRINTERS

Ahmed H. Eid, Brian E. Cooper, and Mohamed N. Ahmed

Lexmark International Inc.
Lexington, KY, USA

ABSTRACT

Ghosting is a common print defect in electrophotographic printing. Printers experiencing ghosting defects show repeated images (residual images) of previously printed contents in the paper process direction. Detecting the residual image (ghost) location and contrast provides necessary information about the ghosting source and severity. In this paper, we present a new system for detecting and quantifying the ghosting defect. It includes a design for a printed test pattern to emphasize the ghosting defect and facilitate further processing and analysis. Wavelet filtering and a template matching technique are used to detect the ghost location along and across the scanned test pattern. A new metric is developed to quantify ghosting based on its contrast, shape, and location consistency. Experimental results on 31 samples of various types of ghosting showed 0.95 correlation between the proposed method's ranking and experts' visual ranking.

Index Terms— Defect, print, ghosting, wavelets, correlation

1. INTRODUCTION

Printer non-uniformity is a common source of print quality degradation. Printers experiencing these kinds of defects show abnormal tone variations, most visibly in large printed areas intended to have constant tone. Examples of printer non-uniformities include banding, jitter, streaking, grain, and mottle [1, 2].

Some types of printer non-uniformities occur only when triggered by certain types of printed content. Specifically, very light or very dark printed areas can cause subsequent content to print either lighter or darker (producing residual images). A *positive* residual image occurs when it matches the previous content (i.e., lighter content caused by a very light area or darker content caused by a very dark area). A *negative* residual image occurs when the residual image is the opposite of the previous content. In either case, these residual images are called *ghosts*, and this type of non-uniformity is called *ghosting*; see Figure 1.

The content-dependent non-uniformity may occur either periodically, at a certain distance from the original content, or once, immediately after (adjacent to) the original content. Only the former effect, called ghosting, will be discussed here. (Halos are an example of the latter effect, appearing along the border of a region.) With ghosting, the residual image occurs at a particular period, based on the circumference of the responsible component (e.g., photoconductor (PC) drum, developer roller). In [3, 4], it is shown that either longer toner charging time or smaller toner diameter can produce ghosting even when using low-resistance developer rollers.

Efficient characterization of print ghosting is essential for fixing the sources of the defect. In [5], a commercially available image analysis camera-based system detects and quantifies ghosting using Fourier analysis. Again, spectral analysis is employed to detect ghosting in [6]. A ghosting index that reflects the ghost contrast and sharpness is introduced in [6] as well. Ghosting test patterns are developed in [5]-[7]. All of these test patterns use rectangular shaped ghost templates. Unfortunately, other print defects (e.g, banding, streaking, PC clouding) can appear simultaneously and interfere with the ghosting defect. In addition, noise and halftone patterns limit the efficacy of simple Fourier analysis in detecting print ghosting, as in [5, 6].

In this paper, we propose a new system for detecting and quantifying ghosting. It includes a design of a new test pattern and a new method for detecting and quantifying ghosting. The test pattern has various flat field (constant coverage) areas and high contrast *unique-shape* ghost templates, for better visibility and detection of the ghost defect based on the shape. The ghost detection relies on wavelet-based filtering and template matching criteria. Wavelets filter out unwanted noise and halftone patterns. A template matching step is then applied to detect both the ghost position and type and measure its shape similarity. The proposed metric combines these quantities along with the contrast to provide a high correlation with the visual assessment of the ghosting defect.

This paper is organized as follows. Section 2 describes the system setup, the test pattern design and the proposed algorithm for detecting and quantifying ghosting. Section 3 provides experimental results on 31 test cases of different ghosting types and severity. Section 4 provides the conclusions.

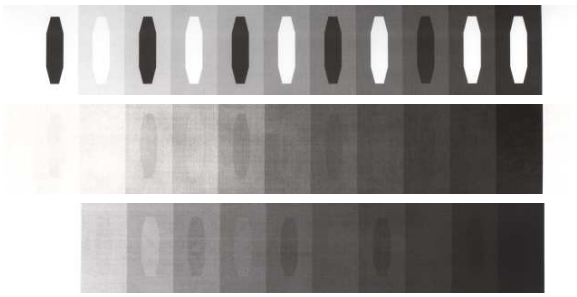

Fig. 1. The black and white ghost templates (top) can induce either positive (center) or negative (bottom) ghosting at a subsequent location on the printed test page.

2. GHOSTING CHARACTERIZATION

2.1. System Setup and Test Pattern Design

The system setup utilizes a scanner system with an automatic belt-fed document feeder. The feed mechanism of this scanner places the sample on the flatbed before scanning. As compared to more conventional paper-fed document feeders, this method introduces less distortion to the scanned image.

The test pattern, shown in Figure 2, consists of 11 flat field (constant coverage) areas, ranging from 0% to 100% coverage in steps of 10%. Black and white "keys" (templates) of a unique symmetric shape appear above and below each flat field area, to emphasize the ghosting defect regardless of printer feed direction. The presence of both black keys and white keys, along with a wide range of constant coverages permits better analysis of both negative and positive ghosting cases and facilitates the comparison between different printers. (Different printers can easily produce different L^* values for the same constant coverage.)

The test pattern image is halftoned and printed at 600 dpi. The printout is then scanned at 600 ppi and calibrated to provide the L^* data for analysis.

2.2. Wavelet-based Filtering

Here, the main concern is the detection of an individual artifact while filtering out other artifacts and unwanted noise. In ghosting detection, wavelets filter out high frequency noise and halftone patterns while retaining the details of certain other frequencies.

This application needs three steps of wavelet processing: decomposition, editing, and reconstruction. The 2D discrete wavelet representation is computed by applying a separable filter bank to the image $I(x, y)$ of size $M \times N$ as:

$$W_\varphi(j_0, m, n) = \frac{1}{\sqrt{MN}} \sum_{x=0}^{M-1} \sum_{y=0}^{N-1} I(x, y)\varphi_{j_0,m,n}(x, y) \quad (1)$$

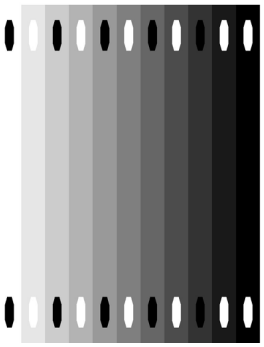

Fig. 2. The test pattern consists of 11 flat field (constant coverage) areas, ranging from 0% to 100% coverage in steps of 10%. The black and white keys are distributed across this range of gray levels to emphasize the ghosting defect.

$$W_\psi^i(j, m, n) = \frac{1}{\sqrt{MN}} \sum_{x=0}^{M-1} \sum_{y=0}^{N-1} I(x, y)\psi_{j,m,n}^i(x, y) \quad (2)$$

where j_0 is an arbitrary starting scale. $\varphi(x, y)$ and $\psi^i(x, y)$, $i \in \{H, V, D\}$ are 2D scaling and wavelet functions, respectively [8]. The $W_\varphi(j_0, m, n)$ coefficients define an approximation of $I(x, y)$ at scale j_0. The details of $I(x, y)$ at scales $j \geq j_0$ are $W_\psi^H(j, m, n)$, $W_\psi^V(j, m, n)$, and $W_\psi^D(j, m, n)$.

The reconstructed ghost image $I^G(x, y)$ contains the vertical and horizontal details of certain frequencies while the diagonal and the approximation components are removed:

$$I^G = \frac{1}{\sqrt{MN}} \sum_{i \in \{H,\ V\}} \sum_{j=j_0}^{\infty} \sum_{m,n} W_\psi^i(i, m, n)\psi_{j,m,n}^i \quad (3)$$

We apply wavelet filtering to both the ghost template (key) image to generate $I^T(x, y)$ and to the flat field area between the upper and lower keys to generate the image $I^G(x, y)$ where the ghosting could appear.

2.3. Template Matching

A sliding sub-image $I^{GW}(x, y) \subset I^G(x, y)$ is matched with $I^T(x, y)$ based on the 2-D correlation score $\rho_f(\cdot)$, where f refers to the percentage fill of each flat field area:

$$\rho_f(i) = \frac{\sum_x^{M_T} \sum_y^{N_T} (I_o^T(x, y))(I_o^{GW_i}(x, y))}{\sqrt{(\sum_x^{M_T} \sum_y^{N_T} I_o^T(x, y)^2)(\sum_x^{M_T} \sum_y^{N_T} I_o^{GW_i}(x, y)^2)}} \quad (4)$$

where $i = 1, 2, .., (M - M_T)$, $I_o^T(x, y)$ and $I_o^{GW}(x, y)$ are zero mean images, $M_T < M$, $N_T < N$ and $\rho_f(i) \in [-1,\ 1]$. For each flat field, the maximum correlation score $\rho_{max}(f)$ is computed as:

$$\rho_{max}(f) = \max_{1 \leq i \leq (M - M_T)} |\rho_f(i)| . \quad (5)$$

At the maximum correlation score, the sign of $\rho_f(i)$ determines whether the ghosting is positive or negative, and the value of i indicates the location of the ghost. The source of the ghost (e.g., due to the PC drum or developer roller) is then determined from the ghost location. Figure 3 shows an example of the detection process for a negative ghosting case.

2.4. Ghost Quantification

To quantify the ghosting severity, we developed a ghosting score that relies on three factors: (1) the ghosting contrast (against the background), (2) the maximum correlation (which depends on the shape of the ghost), and (3) the ghost location consistency. The last two factors serve mainly as a way to reject noise and reduce the false positive rate.

To find the contrast, the ghost should be segmented from the background. The geometry of the ghost shape can be extracted from a ghost template. (Of the templates, we choose the one with the least noise and highest contrast, which usually occurs with the upper left key.) Figure 4(a) shows a template ghost, with its geometry extracted by differentiating the horizontal and vertical profiles of the template to determine the bounding box of the key ghost. The other lines can be determined using a priori information about the ghost shape. Since the template ghost matches the detected ghost, the detected ghost should have the same geometry as the template key; see Figure 4(b).

The difference between the average gray level of the segmented ghost, $g_{in}(f)$, and the average gray level of the background, $g_{ex}(f)$, is used to represent the ghosting contrast; see Figure 4(c). The ghost score (GS) is expressed as:

$$GS = C_{max} \times F(\rho_{max}(f_{C_{max}})) \times P \qquad (6)$$

where $C_{max} = \max_f |g_{ex}(f) - g_{in}(f)|$, and $F(\cdot)$ is a monotonic increasing function of the correlation at $f_{C_{max}}$, the percentage coverage which registered the maximum contrast ghost, C_{max}. The scalar P is less than 0.75 when the ghost locations are inconsistent across the page and unity otherwise.

3. EXPERIMENTAL RESULTS

Thirty-one print samples of different halftoning techniques (classical, stochastic, and Bayer screens) are used throughout this experiment. Voltages in the transfer and development components of the printing mechanism were altered to stress the ghosting defect and to show both negative and positive ghosts. Samples were printed at 600 dpi and then scanned at 600 ppi using a scanning system having an automatic belt-fed document mechanism.

Debauchies wavelets of order 8 were applied to each sample. Horizontal and vertical details of wavelet levels 6, 7 and 8 are kept, while discarding all diagonal and the approximation components. This filtered out the unwanted noise and halftone patterns. In addition, the reconstructed images had minimal dependence on the gray level of both template and ghosts in flat field areas. This helps in subsequent ghost detection.

After detection, the ghosting score quantifies the defect from the original input images. Using the ghosting score (GS), we ranked the 31 samples based on the severity of the ghost, as shown in Figure 5 (top). Independently, print quality experts visually ranked the same print samples. A comparison of the proposed metric ranking and the visual ranking is shown in Figure 5 (bottom). The Spearman's rank correlation coefficient provided 0.95 correlation between both sets of rankings.

Figure 6 shows several detected ghosts from a subset of the examined samples, sorted from left to right, top to bottom based on the ghosting score (GS) provided under each ghost image. As shown, the metric's ranking provides high consistency with a visual assessment.

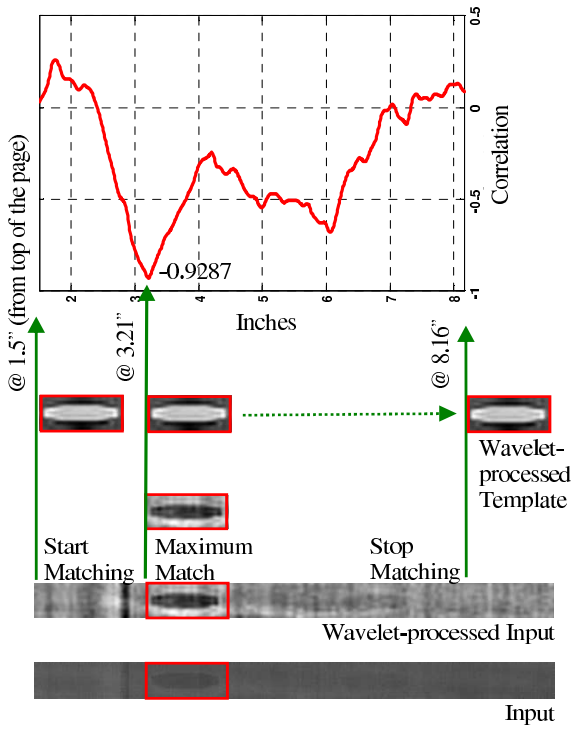

Fig. 3. Ghost detection: for each flat field, the wavelet processed template is matched with a moving window across an area that potentially contains a ghosting defect.

4. CONCLUSIONS

This paper presents a technique for detecting and quantifying ghosting defects in electrophotographic printers, including a design of a test pattern that contains several black and white templates of a specific shape. Flat field areas of various per-

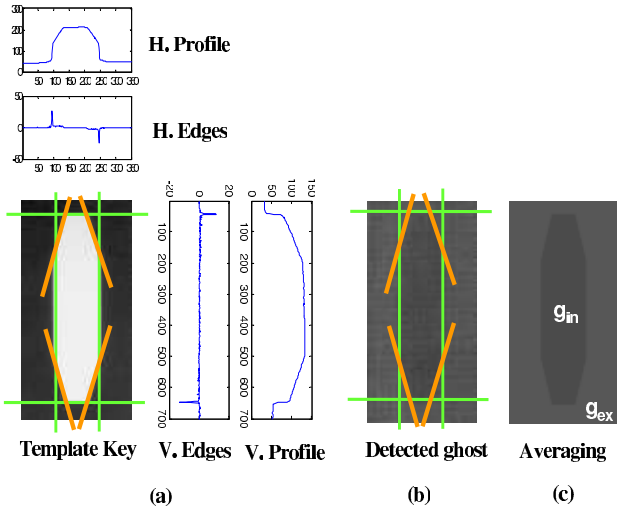

Fig. 4. Ghost quantification: (a) extract ghost geometry from a template ghost, (b) match ghost geometry of the template to the corresponding detected ghost, (c) extract the ghosting contrast from the difference of average interior (g_{in}) and exterior (g_{ex}) intensities of the detected ghost.

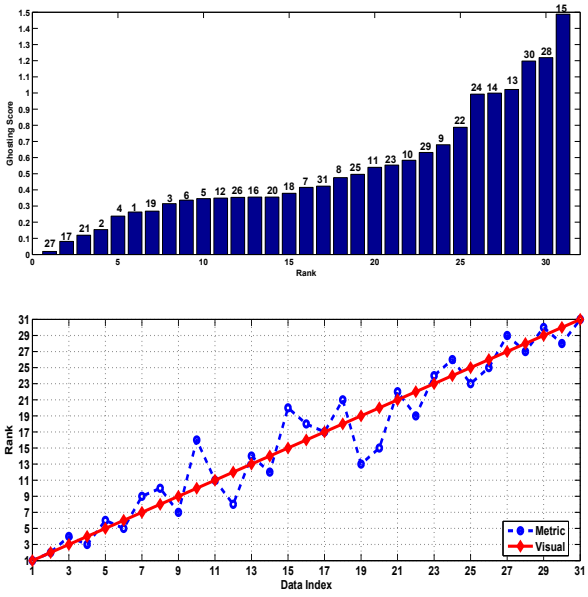

Fig. 5. Ranking of print samples: (top) metric's ranking, (bottom) comparison between metric's ranking and visual ranking by experts.

centage coverages are printed underneath the templates to reveal the ghosting defect.

Wavelets filter out noise and halftones patterns while enhancing the edges of the detected ghosts. A template matching process extracts the predominant ghosts. A ghosting score is presented that reflects the ghosting contrast, the correlation with template shape, and the consistency of ghost location across the different flat field areas.

Experimental results on 31 samples of different strengths of the ghosting defect show 0.95 correlation between the proposed metric and a visual ranking of print quality experts.

5. REFERENCES

[1] D. Rene Rasmussen, Edul N. Dalal and Kristen M. Hoffman, "Measurement of macro-uniformity: streaks, bands, mottle and chromatic variation," *Proc. of IS&T's PICS*, pp. 90-95, Montréal, April 2001.

[2] A. Eid, B. Cooper, and E. Rippetoe, "A unified framework for physical print quality," *Proc. SPIE,* Vol. 6494, Jan. 2007.

[3] T. Iwamatsu, N. Azuma and T. Takaya, "Ghost mechanism of single-component contact development," *Proc. IS&T NIP 14*, pp. 413-416, 1998.

[4] T. Takaya, T. Iwamatsu and N. Azuma, "The characteristics of ghost mechanism in a non-magnetic single component process depends on a diameter of the toner particle," *Proc. IS&T NIP 14*, pp. 422-424, 1998.

[5] J. C. Briggs, E. Hong, and D. Forrest, "Analysis of ghosting in electrophotography," *Proc. IS&T NIP16,* pp. 403-407, 2000.

[6] P. L. Jeran and N. Burningham, "Measurement of electrophotographic ghosting," *Proc. PICS,* pp. 80-83, 2001.

[7] W. Jang, M.-C. Chen, J.P. Allebach, and J Santay, "Print quality test page," *IS&T JIST*, Vol. 48, No. 5, pp. 432-446, Sep./Oct. 2004.

[8] Rafael C. Gonzalez and Richard E. Woods, *Digital Image Processing*, 2nd edition, Prentice Hall Inc., 2002.

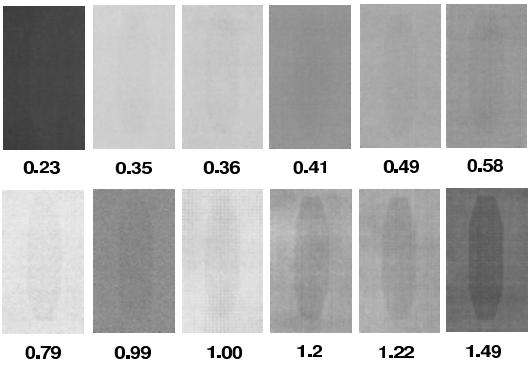

Fig. 6. Selected samples sorted according to the ghosting score (low to high) provided by the proposed algorithm.